

RESEARCH ARTICLE

Physiological adaptation of *Corynebacterium glutamicum* to benzoate as alternative carbon source – a membrane proteome-centric view

Ute Haußmann¹, Su-Wei Qi², Dirk Wolters³, Matthias Rögner¹, Shuang-Jiang Liu^{2*} and Ansgar Poetsch¹

¹Plant Biochemistry, Ruhr University Bochum, Bochum, Germany

²State Key Laboratory of Microbial Resource, Institute of Microbiology, Chinese Academy of Sciences, Beijing, P. R. China

³Analytical Chemistry, Ruhr University Bochum, Bochum, Germany

The ability of microorganisms to assimilate aromatic substances as alternative carbon sources is the basis of biodegradation of natural as well as industrial aromatic compounds. In this study, *Corynebacterium glutamicum* was grown on benzoate as sole carbon and energy source. To extend the scarce knowledge about physiological adaptation processes occurring in this cell compartment, the membrane proteome was investigated under quantitative and qualitative aspects by applying shotgun proteomics to reach a comprehensive survey. Membrane proteins were relatively quantified using an internal standard metabolically labeled with ¹⁵N. Altogether, 40 proteins were found to change their abundance during growth on benzoate in comparison to glucose. A global adaptation was observed in the membrane of benzoate-grown cells, characterized by increased abundance of proteins of the respiratory chain, by a starvation response, and by changes in sulfur metabolism involving the regulator McbR. Additional to the relative quantification, stable isotope-labeled synthetic peptides were used for the absolute quantification of the two benzoate transporters of *C. glutamicum*, BenK and BenE. It was found that both transporters were expressed during growth on benzoate, suggesting that both contribute substantially to benzoate uptake.

Received: January 14, 2009

Revised: March 15, 2009

Accepted: April 5, 2009

**Keywords:**

Aromatic compounds / Benzoate / *Corynebacterium glutamicum* / Membrane proteomics

1 Introduction

The ability of microorganisms to metabolize various carbon sources is a key advantage during the constant competition

Correspondence: Dr. Ansgar Poetsch, Lehrstuhl fuer Biochemie der Pflanzen, Ruhr Universitaet Bochum, 44801 Bochum, Germany

E-mail: ansgar.poetsch@ruhr-uni-bochum.de

Fax: +49-234-32-14322

Abbreviations: ABC, ATP-binding cassette; FA, formic acid; FDR, false discovery rate; MudPIT, multi-dimensional protein identification technology; PR, ProRata; SC, spectral counting; SIM, single ion monitoring; SIMPLE, specific integral membrane peptide level enrichment; TCA, tricarboxylic acid; XCorr, cross correlation score

for nutrition in natural environments. Various microorganisms have evolved the ability to use a broad spectrum of carbon sources as an evolutionary advantage in the colonization of different environments. Aromatic compounds constitute a highly abundant and important source of carbon and energy, especially in natural environments, as assimilation of lignin and its degradation intermediates is an important step in biogeochemical cycling of carbon. Additionally, there is a growing interest in microbial versatility in the degradation of aromatic compounds, which can be exploited for sustainable bioremediation of industrially contaminated environments.

*Additional corresponding author: Dr. Shuang-Jiang Liu

E-mail: liusj@sun.im.ac.cn

Application of proteomic technology for the analysis of aromatic hydrocarbon degradation has proven to be a valuable tool for the study of physiology of degradative bacterial strains. Among the well-studied species there are several *Acinetobacter* [1–3] and *Pseudomonas* strains [4–9], as well as several mycobacterial [10–14] and rhodococcal species [15–18], which are phylogenetically closely related to *Corynebacterium glutamicum*. So far, most studies addressing aerobic aromatic degradation and adaptation to aromatic carbon sources focused especially on elucidating the aromatic catabolic pathways. Therefore, mostly soluble proteomes were analyzed, predominantly by 2-DE followed by mass spectrometry analysis. Only few studies address membrane proteins, as for example Pessione *et al.*, who analyzed the membrane proteome of *Acinetobacter radioresistens* S13 [2], or Kim *et al.*, who besides the soluble proteins of *Pseudomonas putida* KT2440, also analyzed the proteins from the insoluble fraction [7]. In both studies, 2-DE was used as separation method. In the study of Pessione *et al.*, 23 gel spots were compared between gels from acetate-, phenol- and benzoate-grown cells. From the 23 spots, 11 proteins were identified, among them a Na⁺/H⁺-antiporter and an ATP-binding cassette (ABC)-type sugar transporter induced during growth on phenol and benzoate. Kim *et al.* extracted membrane proteins from the insoluble pellet remaining after centrifugation of disrupted *Pseudomonas putida* cells grown on benzoate. After 2-DE they examined 11 gel spots, from which five proteins with one transmembrane segment and two proteins containing two transmembrane segments were identified. Among these proteins, BenF, a benzoate-specific porin was identified as substrate uptake system [7].

Proteomic analysis of integral membrane proteins, especially with multiple transmembrane segments, is still challenging because of their physico-chemical properties. There is a general agreement that 2-DE is unsuitable for analysis of membrane proteins [19], but during the last years several gel-based separation techniques have been developed for membrane proteins, for example in a recent study by Papisotiriou *et al.*, membrane proteomes of Luria broth-, glucose-, and phenol-grown *Pseudomonas* sp. strain pHDV1 cells were compared using doubled-SDS-tricine-PAGE instead of 2-DE separation. A total of 10 outer membrane proteins and 19 inner membrane proteins was identified during growth on the different carbon sources. Two of the outer membrane proteins, a probable porin and a membrane protein involved in aromatic hydrocarbon degradation, were induced during growth on phenol and could be involved in substrate uptake [20].

Regarding the limitations of gel-based approaches, a number of gel-free LC-MS techniques have been developed, often yielding higher coverage of the membrane proteome than gel-based methods. Applying their Specific Integral Membrane Peptide Level Enrichment (SIMPLE)-Multidimensional Protein Identification Technology (MudPIT) approach, Fischer *et al.* detected 42% of all predicted

membrane proteins in *C. glutamicum* [21]. In contrast to gel-based approaches, quantitative proteome analysis in a gel-free experiment is even more challenging. Several label-dependent methods, using stable isotope labeling, either metabolically [22, 23] or chemically [24, 25], as well as label-free techniques, such as spectral counting (SC) [26] or \sum XCorr (sum of peptide SEQUEST XCorr) [27], have been developed. Regarding anaerobic aromatic degradation, one gel-free and quantitative analysis of the membrane proteome exists, which was performed for the *p*-coumarate metabolism in *Rhodospseudomonas palustris*. Pan *et al.* used ¹⁵N metabolic labeling and ProRata (PR) software to comprehensively quantify membrane (and also cytoplasmic) proteins [28]. In contrast to anaerobic degradation of aromatic substrates, no global quantitative model for the adaptation of any bacterial membrane proteome to aerobic degradation of aromatic compounds exists so far. *C. glutamicum*, a Gram-positive, GC-rich, nonsporing, nonmotile soil bacterium extensively used for the fermentative production of fine chemicals, particularly L-glutamate and L-lysine [29], represents a suitable model organism to investigate the adaptation of the membrane proteome to aerobic degradation of aromatic compounds: Growth of *C. glutamicum* on different carbon sources has been extensively analyzed in the past with targeted, and more recently also with global approaches (transcriptomics [30–32], proteomics [33, 34], metabolomics [35, 36]). In the last years, it was shown that *C. glutamicum* is not restricted to sugars or aliphatic acids as carbon sources, but can aerobically catabolize several aromatic compounds. The aromatic catabolic pathways for monocyclic compounds, such as benzoate, gentisate, protocatechuate, *p*-cresol, and resorcinol, have been investigated on the genomic level (reviewed by Brinkrolf *et al.* [37]) and the role of degradative enzymes and transporters has been elucidated [38–41]. Recently, the proteome profiles of *C. glutamicum* grown on benzoate, *p*-cresol, phenol, and resorcinol with a focus on cytosolic proteins involved in aromatic degradation and central carbon metabolism were obtained. This work revealed specific changes in enzyme amounts in central carbon metabolism for each aromatic compound and disclosed the strict requirement of fructose-1,6-bisphosphatase for growth on aromatic hydrocarbons [42].

Although the degradation of aromatic carbon sources by *C. glutamicum* and their impact on central carbon metabolism is well understood, up to now, only scarce information exists about the dynamic adaptation of the bacterial membrane proteome in general and about adaptation to aromatic carbon sources in particular. However, membrane proteins fulfill important cellular functions, such as transport processes or signal transduction, necessary for adaptation to changing environmental conditions [43]. Therefore, the aim of this study was to compare the membrane proteomes of glucose- and benzoate-grown *C. glutamicum* RES167 cells quantitatively using ¹⁵N metabolic labeling and the gel-free SIMPLE-MudPIT technology [21]. Special

focus was on the two benzoate transport proteins BenK and BenE, as their expression was investigated both at mRNA and protein level. The comparison further revealed changes in different functional groups of membrane proteins, such as energy metabolism, transport, cell wall biosynthesis, and sulfur metabolism.

2 Materials and methods

2.1 Cultivation of *C. glutamicum*

C. glutamicum RES167 cells were grown aerobically at 30°C in mineral medium [41] with a rotary shaker, and with 4 mM benzoate or glucose as sole carbon source. For proteome analysis, overnight cultures in 10 mL Luria broth were inoculated into 200 mL mineral medium. The cultures were harvested in the late exponential growth phase (OD_{600nm} of 0.7–0.9).

For the isotopically labeled internal standard, cells were grown on modified MMES medium [44]. Benzoate (10 mM) was added to cover both benzoate- and glucose-specific proteins with the internal standard. Cells were harvested in the exponential growth phase.

2.2 RNA preparation and RT-PCR assays

For the preparation of total RNA, *C. glutamicum* strain RES167 and its mutants ($\Delta benK$, RES167- $\Delta NCgl2325$, and $\Delta benE$, RES167- $\Delta NCgl2326$ [41]) were cultivated in mineral medium with 4 mM glucose or 4 mM benzoate as the sole source of carbon and energy. Exponentially growing cells (optical density at 600 nm of 0.7) were harvested by centrifugation at 11 000 $\times g$ for 5 min. Subsequently, the supernatant was decanted, and the pellet was transferred into liquid nitrogen. RNA isolation was performed with a TRNzol RNA Reagent Kit (TIANGEN, Beijing, China) as indicated by the manufacturer. The extracted RNA was dissolved in 50 μ L water. Residual DNA was removed by treatment with 10 U DNase I (RNase free) (TaKaRa, catalog no. D2215) and 40 U of RNase inhibitor (TaKaRa, catalog no. D2310A) for 30 min at 37°C.

RT-PCR assays were performed by using M-MLV RT (Promega, USA) and primers specific for the desired genes

Table 1. Primers used for gene amplification in this study

Name	Sequence (5' \rightarrow 3')	Reference
<i>NCgl2325R</i>	GATGAGGAATGCGGAGCTTGGTCC	This study
<i>NCgl2325F</i>	GATTTCGCTGGAATTTTCTCCTCCAAG	This study
<i>NCgl2326R</i>	GATTCCGAGGATGCTGATTTCCGAC	This study
<i>NCgl2326F</i>	GAACCATCGTTGCCATCGCATCCG	This study
1492R	GGTTACCTTGTTACGACTT	Lane <i>et al.</i> [86]
27F	AGAGTTTGATCCTGGCTCAG	Lane <i>et al.</i> [86]

(Table 1) according to the protocol from Liu *et al.* [45]. To ascertain that no residual DNA was present in the RNA preparations, a PCR without RT was performed with the same primers and conditions.

2.3 Preparation of membranes

C. glutamicum RES167 cells were harvested by centrifugation for 15 min at 4500 $\times g$; cells were washed with PBS (137 mM NaCl, 2.7 mM KCl, 10 mM Na₂HPO₄, 1.8 mM KH₂PO₄, pH 7.4) and resuspended at a concentration of 10 mL disintegration buffer/g wet cells (PBS containing additional 20 mM MgCl₂, 10 mM MnCl₂, 200 U/mL DNaseI, protease inhibitor mix for bacterial cells (Sigma, St. Louis, MO, USA)). Disruption of cells was done by a French Pressure Cell (40K cell with a volume of 35 mL, Thermo Spectronic, Rochester, USA) with four passages at 20 000 psi. Unbroken cells and cell debris were sedimented twice by centrifugation at 5000 $\times g$ and 4°C. Membranes were enriched by ultracentrifugation at 100 000 $\times g$ and 4°C for 30 min. The resulting pellet was resuspended gently with ice-cold PBS and ultracentrifugation was repeated. Membranes were stored in PBS with 10% glycerol and protease inhibitors at –70°C.

2.4 Digestion of membranes

Isolated membranes from *C. glutamicum* ¹⁴N samples (grown on 4 mM benzoate or glucose) were pooled with membranes of equal protein amounts of the internal ¹⁵N standard (grown on benzoate and glucose as mixed carbon sources). A total protein content of 500 μ g was digested according to the SIMPLE protocol [21]. The products of the tryptic predigest in aqueous solution as well as of the combined trypsin/chymotrypsin digestion (SIMPLE) were depleted of membrane fragments and undigested proteins by centrifugation at 100 000 $\times g$ (30 min, 4°C) and desalted using Spec PT C18 AR solid phase extraction pipette tips (Varian, Lake Forest, CA, USA).

Products of both digestion steps were analyzed, as proteins identified in predigest and SIMPLE are complementary. In the predigest especially hydrophilic segments of membrane proteins are digested, as well as membrane-associated and cytoplasmic proteins present in the membrane sample. On the contrary, the SIMPLE digest addresses hydrophobic parts of membrane proteins, while the membranes should already be depleted from cytoplasmic and membrane-associated proteins.

2.5 MudPIT

The desalted samples were loaded onto a triphasic microcapillary packed as described in Fischer *et al.* [21]. MudPIT was performed using an Accela gradient HPLC pump

system (Thermo Electron) coupled to an LTQ Orbitrap mass spectrometer (Thermo Electron). The LTQ Orbitrap was operated *via* instrument method files of Xcalibur (Rev. 2.0.7). The linear ion trap and the orbitrap were operated in parallel, *i.e.* during a full MS scan on the orbitrap at a resolution of 60 000, MS/MS spectra of the four most intense precursors were detected in the ion trap. The heated desolvation capillary was set to 200°C. The relative collision energy for collision-induced dissociation was set to 35%. Dynamic exclusion was enabled with a repeat count of 1 and a 1 min exclusion duration window. Singly charged and more than triply charged ions were rejected from MS/MS. The column flow rate was set to ~250 nL/min and a spray voltage of 1.5–1.8 kV was applied. The four buffers used for the chromatography were 2% ACN, 0.1% formic acid (FA) (buffer A), 80% ACN, 0.1% FA (buffer B), 0.25 M ammonium acetate, 0.1% FA (buffer D), and 1.5 M ammonium acetate, 0.1% FA (buffer C). Before the salt steps, a linear gradient of 0–100% buffer B in 180 min was applied and each salt step was followed by a linear gradient of buffer B in 110 min. For predigest samples 5, 10, 20, 30, 50, and 90% of buffer D, followed by 50 and 100% of buffer C were used to displace fractions from the cation exchanger onto the reversed phase material. Finally, a 10 min salt wash with 100% buffer C was performed. For SIMPLE measurements salt steps of 0% buffer D (240 min), 5% buffer D (180 min), 10% buffer D (180 min), 50, 70, and 100% buffer D (130 min each) were applied, followed by 100% buffer C and the final salt wash (130 min each).

2.6 Database searches

All database searches were performed using SEQUEST algorithm, embedded in Bioworks™ (Rev. 3.3, Thermo Electron © 1998–2006), with a *C. glutamicum* ATCC 13032 Bielefeld database containing 3058 sequences, which was provided by Kalinowski *et al.* [46]. A similar *C. glutamicum* database is available at EBI proteomes [47]. Strain RES167 is a restriction-deficient mutant of the wild type strain ATCC 13032 [48].

As no splice variants or protein isoforms exist in bacterial strains, such redundancies were not taken into account. The selected enzyme specificities were different for predigest and the SIMPLE samples. For predigest samples only tryptic peptides with up to two missed cleavages were accepted, while for SIMPLE samples no enzyme specificity was considered. All other search parameters were the same for all samples: No fixed modifications were considered. Oxidation of methionine was permitted as variable modification. The mass tolerance for precursor ions was set to 10 ppm; the mass tolerance for fragment ions was set to 1 amu.

For protein identification, a threshold for both protein and peptide probability was set to 0.001, and at least two different peptides *per* protein were required. For an esti-

mation of the false discovery rate (FDR), a reversed database [49] generated in Bioworks™ was searched, containing the reversed protein sequences from the original database. The FDR was calculated by dividing the absolute number of hits from this reversed database through the sum of hits from both database searches (reversed database and actual database). FDR was estimated using two different sets of filter criteria: (i) filter 1 for protein identification and SC (protein and peptide probability ≤ 0.001 and ≥ 2 different peptides per protein); (ii) filter 2 for PR quantification (difference in cross correlation score ≥ 0.08 ; XCorr ≥ 1.8 (+1), 2.5 (+2), 3.5 (+3); ≥ 2 different peptides *per* protein). FDR for protein identification was determined for both sets of filter criteria and was below 1% for both filters and both predigest and SIMPLE measurements.

2.7 Relative quantification by ProRata 1.1

Since an internal standard was used for relative protein quantification, benzoate and glucose samples were compared indirectly: Using ProRata software [50], peak areas of unlabeled ^{14}N peptides (from benzoate or glucose samples) and of isotopically labeled ^{15}N peptides (from the internal standard) can be calculated. Following PR analysis abundance ratios for the comparison of the ^{14}N benzoate and the ^{14}N glucose samples can be determined by dividing the regulation factors obtained for benzoate: standard and glucose: standard – a strategy suggested earlier by MacCoss *et al.* for RelEx [51].

Prior to PR analysis, DTA and OUT files were generated from search results files using Bioworks software (Thermo Electron) and filtered using DTAslect 1.9 software [52] with the following parameters: minimum difference in cross correlation score was set to 0.08, minimum XCorr was set to 1.8 (+1), 2.5 (+2), 3.5 (+3), and duplicate spectra for each sequence were retained ($-t$ 0). Raw-files were converted to mzXML files using the raw2mzXML-tool embedded in PR. Estimation of protein abundance ratios was performed by PR 1.1 software [50] using default parameters, but adding oxidation of methionine as variable modification. The PR default parameters comprise a threshold of at least two peptides *per* protein used for the calculation of the protein abundance ratio. From all regulation factors (\log_2 ratios) obtained in one measurement, the median was calculated. As most proteins in the sample are not expected to change in their abundance, the median of the regulation factors should be 0. If the observed median differed from 0, the difference was added to or subtracted from all regulation factors of the measurement. The normalized regulation factors (sample compared with internal standard) from three biological replicates, consisting of one benzoate and one glucose sample, were analyzed by student's *t*-test. Proteins with a *p*-value < 0.05 were considered significantly regulated. From the regulation factors of benzoate/internal standard and glucose/internal standard, the ratio for

benzoate to glucose was calculated by division of the two factors, *i.e.* subtraction of the \log_2 ratios.

2.8 Relative quantification by spectral counting

Criteria for protein identification were set to a peptide and protein probability <0.001 and at least two peptides *per* protein. MS^2 spectra *per* protein were counted from BioworksTM result tables using an in-house Perl script. Spectral counts of the different samples were normalized by dividing the number of spectra of each protein by the sum of all spectra in the sample and multiplying the result with the sum of spectra of the sample with the fewest spectra. The \log_2 of the individual spectral counts was calculated and the results from the benzoate and the glucose samples were statistically analyzed by student's *t*-test. Proteins were considered significantly regulated if the *p*-value was <0.05 , if at least five spectra were detected per sample (in all three benzoate or all three glucose samples).

2.9 Assessment of false positive rate for protein quantification

To estimate the false positive rate for protein quantification, a volcano plot [53] was drawn (see Supporting Information Figs. 1 and 2): the *p*-values of all quantified proteins from predigest and SIMPLE digest samples were plotted against the regulation factors as \log_2 ratios. Additionally to the experimentally obtained dataset, a permuted dataset was constructed by shuffling the values from benzoate and glucose samples randomly. The *t*-test was repeated for the permuted dataset and the data points were included into the volcano plot. A cutoff in *p*-value can be defined and the false positive rate can be determined as the number of permuted data points exceeding the cutoff divided by the sum of the number of experimental data points plus the number of the permuted data points exceeding the same cutoff. For a *p*-value cut-off of 0.05, a false positive rate of 19% was determined for quantification with PR and of 45% for quantification using spectral counts.

2.10 Absolute quantification of the benzoate transport proteins BenK and BenE

For absolute quantification of the benzoate transport proteins BenK and BenE, stable isotope-labeled synthetic peptides were spiked to SIMPLE digests of membranes of benzoate-grown cells from biological replicates 1 and 3. The peptide sequences used for the design of the synthetic peptides were chosen from the sequences identified from MS/MS scans in SIMPLE measurements for BenK and BenE. For BenK, the peptide IGA[L]SAGAVGDR was chosen, for BenE the peptide LASIAPPVAVAAVVG[IT]

VAIASGK was chosen as reference peptide. Labeled peptides were purchased from Thermo Scientific. The marked L or I residues contained 1^{15}N and 6^{13}C , yielding a mass difference of 7 amu to the unlabeled peptide. Labeled peptides of 400 fmol were spiked to 500 μg of membranes of benzoate-grown cells from different biological replicates, digested according to the SIMPLE protocol. The desalted samples were loaded onto a triphasic microcapillary column packed as described in Fischer *et al.* [21]. MudPIT was performed using an Accela gradient HPLC pump system (Thermo Electron) coupled to an LTQ Orbitrap mass spectrometer (Thermo Electron). The LTQ Orbitrap was operated *via* instrument method files of Xcalibur (Rev. 2.2). Single ion monitoring (SIM) scans were measured with the Orbitrap for scan ranges (i) 1085–1098 *m/z*, (ii) 540–550 *m/z*, and (iii) 723–733 *m/z* at a resolution of 30 000. In parallel, MS/MS scans were performed in the linear ion trap, using parent masses of (i) 1088.16 *m/z*, (ii) 543.80 *m/z*, and (iii) 725.78 *m/z* (with iso width = 2 *m/z*, collision energy = 35%, act. time = 30 ms). The solvent gradients applied were the same as for the SIMPLE digests described above. All database searches were performed using SEQUEST algorithm, embedded in BioworksTM (Rev. 3.3.1 SP1, Thermo Electron © 1998–2007), with a *C. glutamicum* ATCC 13032 Bielefeld database containing 3058 sequences, which was provided by Kalinowski *et al.* [46]. SIM scans, in which the unlabeled peptides were detected (filter criteria: peptide and protein probability ≤ 0.001), were used for quantification. The sums of peak intensities (corresponding to the respective isotopologues) were calculated for the unlabeled and the labeled peptide for both transport proteins. Division of the ratios unlabeled/labeled of the BenE and BenK peptide yields the abundance ratio of BenE/BenK in the sample.

3 Results

3.1 General profiles of membrane proteomes of benzoate- and glucose-grown cells

For the genome of *C. glutamicum* ATCC 13032 3058 protein coding regions have been predicted (CoryneRegNet) [54]. The strain RES167 used in this study is a restriction deficient mutant of ATCC 13032 with the same genetic background [48]. Twenty-one percent (about 650) of all genes code for integral membrane proteins according to predictions of TMHMM v2.0 [55]. Peptide and protein probabilities of 0.001 and smaller and at least two different peptides *per* protein were set as criteria for protein identification. According to these criteria, a total of 794 proteins were identified (see Supporting Information Tables 1 and 2), 495 proteins were identified both in benzoate- and glucose-grown cells, while 92 and 207 proteins were detected exclusively in benzoate- or glucose-grown cells. Almost one-third of all identified proteins were annotated as integral

membrane proteins (benzoate-grown cells: 31%; glucose-grown cells: 29%), another 13% were annotated as secreted proteins. In total, 242 (38% of all predicted) integral membrane proteins were identified. While 146 membrane proteins were found in both benzoate- and glucose-grown cells, 38 proteins were identified only during growth on benzoate and 58 exclusively during growth on glucose.

Grouping of the identified membrane proteins according to function revealed that the proportions of the functional categories of the identified proteins were very similar to the annotations for the complete membrane proteome and that there were only minor differences between the functional distribution of membrane proteins observed during growth on benzoate and glucose (see Fig. 1).

Quantification by metabolic labeling was achieved using PR Software [50]. Hundred ninety-four proteins (24% of all proteins identified) were quantified by PR in all three biological replicates (see Supporting Information Table 3). Another 16 proteins were quantified in either all benzoate- or all glucose-grown samples. Generally, protein quantification by metabolic labeling was judged more accurate than quantification by SC, as it is less dependent on protein size,

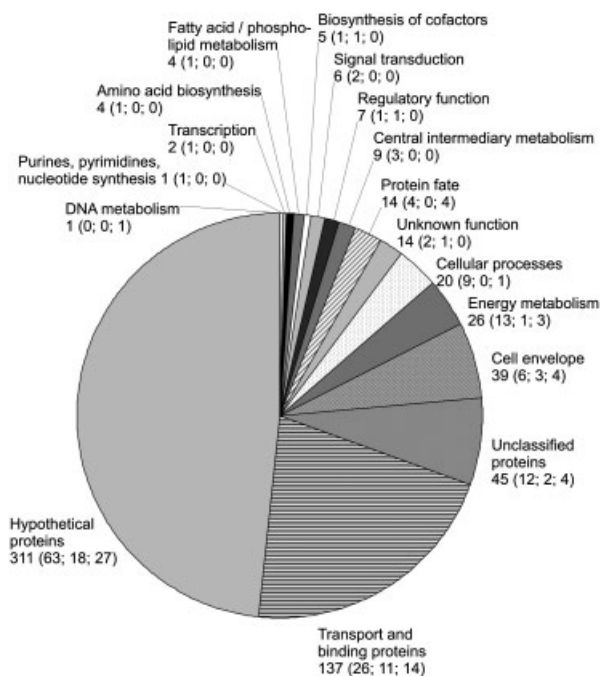


Figure 1. Distribution of all annotated and identified *C. glutamicum* membrane proteins according to their functional category based on the genome annotation of DNA data bank of Japan [85]. All proteins listed were detected with two different peptides, as well as protein and peptide probability-values <0.001 in at least one biological replicate. Numbers in front of the brackets indicate the number of all proteins annotated to the corresponding category. Three numbers within the brackets indicate: Proteins identified in both benzoate- and glucose-grown cells; proteins identified upon growth on benzoate; proteins identified upon growth on glucose.

abundance, enzymatic cleavage sites, or HPLC conditions [56]. Therefore, results of relative quantification of peak areas are given, if available. If quantification by comparison of peak areas was not possible, for example due to missing values, results of SC are given to estimate protein abundance changes. The abundance change of induced proteins, expressed either during growth on benzoate or glucose, was estimated by SC, for example for all gene products of the *ben* gene cluster. (For a comparison of PR and SC results, see Supporting Information Table 4.) Table 2 lists all significantly regulated proteins and the method of quantification used for each protein. For two proteins, Cg1367 and Cg3404, which were significantly regulated according to SC, no significant regulation was detected by PR. Therefore, these proteins were excluded from Table 2.

3.2 Substrate uptake systems

The most pronounced differences between benzoate- and glucose-grown cells were detected in the group of transport proteins. Special focus was given to the substrate uptake systems both for benzoate and glucose. *C. glutamicum* possesses two benzoate transporters, BenK (Cg2642) and BenE (Cg2643) [41]. Up to now there is no knowledge about possible functional or regulatory differences between the two transporters. Both benzoate transporters were identified exclusively in the membranes of benzoate-grown cells. In contrast to BenK (\log_2 ratio 4.9 (SC)), only few peptides from BenE were detected, thus the threshold criteria for significant quantification were not reached. Besides the transporters, two benzoate-degrading enzymes, BenA (Cg2637) and BenD (Cg2640), and the putative LuxR-type transcriptional regulator of the *ben* gene cluster, BenR (Cg2641) [37], were induced during growth on benzoate (\log_2 ratios from 4.9–5.9 (SC)) (see Fig. 4). In contrast to the benzoate transporters, the glucose-specific enzyme II of the phosphotransferase system (PtsG) was not differentially regulated between glucose- and benzoate-grown cells. Based on the total amount of identified peptides, PtsG was one of the most abundant membrane proteins under both conditions. But PtsS (Cg2925), the sucrose-specific enzyme II of the phosphotransferase system, exhibited decreased abundance in benzoate-grown cells (\log_2 ratio -1.1 ; PR).

Additionally, two ABC-type transport systems, annotated as putative sugar transporters, were upregulated during growth on benzoate: Cg2708 (MsiK1), an ATPase component, as well as Cg0834, a secreted component, and Cg0835 (MsiK2), the corresponding ATPase component, were found to be upregulated by \log_2 ratios of 1.2–1.7 (PR).

3.3 Transcription of *benK* and *benE* in the RES167 strain and *benK* and *benE* deletion mutants

Both benzoate transport proteins, BenK and BenE, were identified in the membranes of benzoate-grown cells, but

Table 2. Proteins differentially regulated during growth on benzoate

ID	Localization	Description	log ₂ ratio	p- value	ProRata		Spectral counts	
					Predigest	SIMPLE	Predigest	SIMPLE
Proteins up-regulated during growth on benzoate								
Cg0446	C	(SdhA) succinate dehydrogenase A	1.5	0.049	x			
Cg0480	C	(FadD5) long chain fatty acid-CoA ligase	1.1	0.007	x			
Cg0596	C	(RplD) 50S ribosomal protein L4	0.8	0.038	x			
Cg0600	C	(RplV) ribosomal protein L22	0.6	0.049	x			
Cg0756	M	(CstA) putative carbon starvation protein A	0.4	0.008	x			
Cg0834	S	Bacterial extracellular solute-binding protein	1.7	0.020	x	X		
Cg0835	C	(MsiK2) ABC-type sugar transport system	1.4	0.008		x		
Cg0952	M	Putative integral membrane protein (<i>cg0952</i> is co-transcribed with <i>mctC</i> [63])	0.7	0.037	x			
Cg1314	M	(PutP) proline transport system	1.6	0.027	x			
Cg1362	M	(AtpB) ATP synthase F0 Subunit 6	0.4	0.006	x			
Cg1366	C	(AtpA) Probable ATP synthase alpha chain protein	0.4	0.008		x		
Cg1762	C	(SufC) iron-regulated ABC transporter ATPase subunit	0.5	0.013	x			
Cg2136	C	(GluA) glutamate uptake system ATP-binding protein	0.4	0.032		x		
Cg2137	S	(GluB) glutamate secreted binding protein	1.6	0.027	x			
Cg2181	S	ABC-type peptide transport system	1.9	0.014		x		
Cg2184	C	ATPase component of peptide ABC-type transport system	1.5	0.001	x	X		x
Cg2403	M	(QcrB) cytochrome B	1.4	0.009	X	x		
Cg2404	M	(QcrA1) Rieske iron-sulfur protein	1.4	0.009	X	x		
Cg2637	C	(BenA) benzoate 1,2-dioxygenase alpha subunit	5.9	0.004			x	
Cg2640	C	(BenD)1,6-dihydroxycyclohexa-2,4-diene-1-carboxylate dehydrogenase	5.5	0.002			x	
Cg2641	C	(BenR) putative bacterial regulatory protein, LuxR family	4.9	0.008			x	
Cg2642	M	(BenK1) benzoate transport protein	4.9	0.013				x
Cg2708	C	(MsiK1) ABC-type sugar transport system	1.2	0.002	x	X		
Cg3195	C	Flavin-containing monooxygenase (FMO)	2.2	0.007	X		x	
Proteins down-regulated during growth on benzoate								
Cg0012	C	(SsuR) transcription regulator protein	-3.0	0.038			x	
Cg0414	M	(Wzz) cell surface polysaccharide biosynthesis	-0.6	0.009	x			
Cg0417	M	(CapD) probable DTDP-glucose 4,6-dehydratase transmembrane protein	-0.3	0.015	x			
Cg0561	M	(SecE) SecE subunit of protein translocation complex	-0.7	0.047		x		
Cg0736	C	(MetN) ABC-type methionine transporter ATPase subunit	-1.4	0.001	x	X	x	
Cg0791	C	(Pyc) pyruvate carboxylase	-0.5	0.020	x			
Cg1001	M	(MscL) large conductance mechanosensitive channel	-1.0	0.028	x			
Cg1737	C	(Acn) aconitase	-1.6	0.004	x			
Cg1753	C	ATPase component of ABC transporters with duplicated ATPase domains	-0.8	0.036			x	
Cg1806	C	(MetK) S-adenosylmethionine synthetase	-1.6	0.019	x			
Cg2496	S	Putative secreted protein	-0.8	0.005	x			
Cg2810	M	Na ⁺ /H ⁺ -dicarboxylate symporter family	-1.6	0.026				x
Cg2925	M	(PtsS) enzyme II sucrose protein	-1.1	0.042		x		
Cg2964	C	(GuaB1) inositol-monophosphate dehydrogenase	-1.5	0.001	x			
Cg3115	C	(CysD) sulfate adenylyltransferase subunit 2	-2.7	0.009	X		x	
Cg3182	S	(Cop1) trehalose corynomycolyl transferase	-0.4	0.006	x			

The table lists proteins significantly up- or down-regulated during growth on benzoate. Regulation factors obtained with either PR or SC for three biological replicates were submitted to a *t*-test. *p*-values <0.05 were considered significant. Regulation factors are given as log₂ ratios. Besides the protein ID, the localization (C, cytoplasmic; M, membrane integral; S, secreted) and a description of protein function are listed. The four columns following the log₂ ratio show whether the regulation factor displayed was obtained with PR or SC, in a predigest or a SIMPLE measurement. Capital X symbols indicate from which sample the respective regulation factor was calculated.

not in glucose-grown cells. To verify that transcription of *benK* and *benE* is absent during growth on glucose, total RNA of exponentially growing RES167 cells and of deletion mutants of both transporters ($\Delta benK$: RES167- $\Delta NCgl2325$ ($-\Delta 25$; *cg2642*); $\Delta benE$: RES167- $\Delta NCgl2326$ ($-\Delta 26$; *cg2643*)) [41] was isolated and submitted to RT-PCR assays. Figure 2A shows that both transporter genes were transcribed during growth on benzoate in RES167, while during growth on glucose transcription was not detected.

In the deletion mutants, transcription of the remaining transporter was tested. During growth on benzoate, but not on glucose, *benE* was transcribed in the $\Delta benK$ deletion mutant (Fig. 2B, lane E), as well as transcription of *benK* was observed during growth on benzoate in the $\Delta benE$ deletion mutant (Fig. 2B, lane 5).

3.4 Absolute quantification of BenK and BenE

After co-expression of both benzoate transporters was observed both on RNA and protein level, absolute protein quantification was performed to estimate the abundance ratio of BenK to BenE. Therefore, sum of peak intensities (corresponding to the respective isotopologues) of unlabeled peptides of the transport proteins were compared with sum of peak intensities of stable isotope-labeled synthetic peptides specific for BenK and BenE. The results are summarized in Table 3. Analysis of membranes of benzoate-grown cells from the first biological replicate yielded 13 MS/MS spectra of the BenK peptide and 25 MS/MS spectra of the BenE peptide. From 10 of 13 and 24 of 25 corresponding SIM scans, sum of peak intensities were calculated. For BenK, the average ratio of peak intensities of unlabeled to labeled peptides was 0.15 (standard deviation = 0.01). For BenE, the average ratio of peak intensities of unlabeled to labeled peptides was 0.29 (standard deviation = 0.02). Division of the average ratios for BenE and BenK yielded an abundance ratio of 1.93. Analyzing membranes of benzoate-grown cells from the third biological replicate, 35 MS/MS spectra of the BenK peptide and 170 MS/MS spectra of the BenE peptide were detected. Thirty-three of 35 and 168 of 170 corresponding SIM scans were used for quantification.

For BenK, the average ratio of peak intensities of unlabeled to labeled peptides was 0.70 (standard deviation = 0.06). For BenE, the average ratio of peak intensities of unlabeled to labeled peptides was 0.99 (standard deviation = 0.10). Division of the average ratios for BenE and BenK yielded an abundance ratio of 1.41. From these data it can be concluded that, under the digestion conditions chosen, the amounts of BenK and BenE in the membranes of benzoate-grown cells do not differ drastically. BenE appears to be slightly more abundant than BenK. Although the ratios of BenE:BenK were similar in both biological replicates analyzed, the absolute amounts of BenE and BenK differed between the replicates (see Table 3).

3.5 Amino acid transport systems

Besides the substrate uptake systems for benzoate and sugars, several amino acid uptake systems showed abundance differences between the two carbon sources. The proline transporter PutP [57] (Cg1314, \log_2 ratio 1.6 (PR)) and two subunits of the glutamate uptake system GluABCD, the secreted glutamate binding protein GluB [58] (Cg2137, \log_2 ratio 1.6 (PR)) and the ATPase component GluA (Cg2136, \log_2 ratio 0.4 (PR)) were upregulated in benzoate-grown cells, as well as two subunits of a putative peptide transport system, Cg2181 (\log_2 ratio 1.9 (PR)), the secreted component, and Cg2184 (\log_2 ratio 1.5 (PR)), the ATPase component. In contrast to these results, MetN (Cg0736, \log_2 ratio -1.4 (PR)), which was shown to be the ATPase subunit of an ABC-type methionine transporter [59], was downregulated in benzoate-grown cells.

3.6 Other transport proteins

Among the transport proteins that changed their abundance, there are two proteins with unknown function: Cg2810, downregulated by a \log_2 ratio of -1.6 on benzoate (SC), belongs to the Na^+/H^+ -dicarboxylate symporter family. The second protein, Cg1753, is annotated as ATPase-component of an ABC-type transport system. It was downregulated in benzoate-grown cells by a factor of -0.8 (\log_2 , SC).

The third protein in this group (*MscL*) has been characterized as large conductance mechanosensitive channel, an osmo-regulated exporter of compatible solutes in case of hypo-osmotic shock [60]. *MscL* exhibited decreased abundance in benzoate-grown cells (\log_2 ratio -1.0 (PR)). It was shown that transcription of *mscL* was upregulated in a $\Delta mtrAB$ deletion mutant [61]. But a response to changes of osmolality most likely can be excluded, as ProP, BetP, and LcoP, which are positively regulated by MtrAB [62], were not detected.

Additionally, Cg0592 was upregulated by a \log_2 ratio of 0.7 (PR) during growth on benzoate. The *cg0592* gene is co-transcribed with *cg0953*. The Cg0953 protein was recently characterized as an uptake system for monocarboxylic acids and named MctC [63]. An overview of all differentially regulated membrane proteins is given in Fig. 3.

3.7 Changes of cell wall proteins

The cell wall also seems to be affected by the adaptation to growth on benzoate, since three proteins involved in cell wall biosynthesis were found to be slightly downregulated in benzoate-grown cells: Cop1 (Cg3182) (\log_2 ratio -0.4 (PR)) is one of the six mycolyltransferases of *C. glutamicum* attaching mycolic acids to arabinogalactan. It was also shown to influence cell shape [64]. Wzz (Cg0414) (\log_2 ratio -0.6 (PR)) is annotated as cell surface biosynthesis protein/chain length determinant protein. In *E. coli*, Wzz was shown to determine the chain

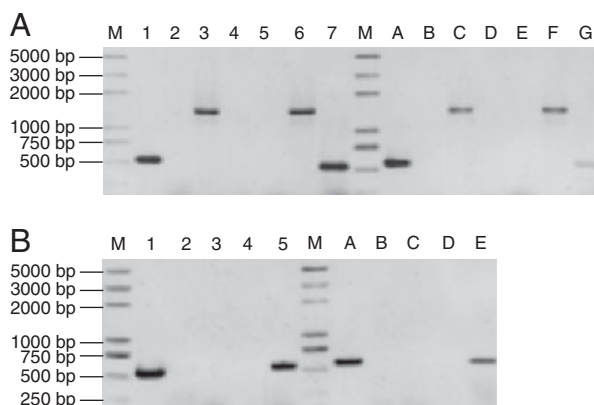


Figure 2. (A) One experiment for the detection of *benK* and *benE* expression using RT-PCR with designed primers. Total RNA was isolated from RES167 grown on mineral medium with 4 mM Glucose (MM+G) or 4 mM Benzoate (MM+B) as sole carbon source, respectively. Lanes 1 and A show the PCR products of the total DNA from RES167 performed with designed primers of *benK* or *benE*. Lanes 2 and B show the PCR products of total RNA from RES167 growing on (MM+G) performed with designed primers of *benK* or *benE*. Lanes 3 and C show the RT-PCR products of the total RNA from RES167 growing on (MM+G) performed with general primers of bacteria. Lanes 4 and D show the RT-PCR products of the total RNA from RES167 growing on (MM+G) performed with designed primers of *benK* or *benE*. Lanes 5 and E show the PCR products of the total RNA from RES167 growing on (MM+B) performed with designed primers of *benK* or *benE*. Lanes 6 and F show the RT-PCR products of the total RNA from RES167 growing on (MM+B) performed with general primers of bacteria. Lanes 7 and G show the RT-PCR products of the total RNA from RES167 growing on (MM+B) performed with designed primers of *benK* or *benE*. Lane M: Marker: DL2000 Plus™ DNA Marker (TransGen Biotech, Beijing). (B) One experiment for the detection of RT-PCR products of *benK* and *benE* from mutants RES167-Δ26 or RES167-Δ25. Total RNA was isolated respectively from RES167, mutants RES167-Δ26 or RES167-Δ25 grown on mineral medium with 4 mM Glucose (MM+G) or 4 mM Benzoate (MM+B) as sole carbon source. Lanes 1 and A: the PCR products of the total DNA from RES167 performed with designed primers of *benK* and *benE* as control. Lane 2: the PCR product of total RNA from RES167-Δ26 growing on (MM+G) performed with designed primers of *benK*. Lane 3: the RT-PCR product of the total RNA from RES167-Δ26 growing on (MM+G) performed with designed primers of *benK*. Lane 4: the PCR product of the total RNA from RES167-Δ26 growing on (MM+B) performed with designed primers of *benK*. Lane 5: the RT-PCR product of the total RNA from RES167-Δ26 growing on (MM+B) performed with designed primers of *benK*. Lane B: the PCR product of total RNA from RES167-Δ25 growing on (MM+G) performed with designed primers of *benE*. Lane C: the RT-PCR product of the total RNA from RES167-Δ25 growing on (MM+G) performed with designed primers of *benE*. Lane D: the PCR product of the total RNA from RES167-Δ25 growing on (MM+B) performed with designed primers of *benE*. Lane E: the RT-PCR product of the total RNA from RES167-Δ25 growing on (MM+B) performed with designed primers of *benE*. Lane M: Marker: DL2000 Plus™ DNA Marker (TransGen Biotech, Beijing).

length of the O-antigen, constituting one region of lipopolysaccharide [65]. CapD (Cg0417) (\log_2 ratio -0.3 (PR)) is predicted to be involved in cell wall biogenesis, too. In *Bacillus anthracis*, CapD was identified to be involved in the covalent anchoring of the polyglutamate capsule to peptidoglycan [66].

3.8 Regulation of proteins involved in oxidative phosphorylation

The change of the carbon source leads to an adjustment of the central carbon and energy metabolism, resulting in an upregulation of the membrane protein complexes of the electron transport chain in benzoate-grown cells (see also Fig. 3): Subunit A of the succinate dehydrogenase (Cg0446) was found to be upregulated (\log_2 ratio 1.5 (PR)), as well as two subunits of the cytochrome bc_1 complex QcrA1 (Rieske iron sulfur protein) Cg2404, \log_2 ratio 1.4 (PR); QcrB (cytochrome B) Cg2403, \log_2 ratio 1.4 (PR). Subunits α (AtpA) and β (AtpB) of the ATP-synthase were identified to be slightly upregulated, too (Cg1366 \log_2 ratio 0.4 (PR); Cg1362 \log_2 ratio 0.4 (PR)).

3.9 Impact on sulfur metabolism

Adaptation to benzoate as carbon source seems to affect sulfur and methionine metabolism. Besides the downregulation of the methionine transporter subunit MetN (Cg0736, \log_2 ratio -1.4), as mentioned above, also MetK (Cg1806, \log_2 ratio -1.6 (PR)), catalyzing the conversion of methionine to S-adenosyl methionine [67], was downregulated during growth on benzoate. Additionally, the transcriptional regulator SsuR (Cg0012), which activates the expression of sulfonate utilization genes in the absence of sulfate [68], was found to be downregulated (\log_2 ratio -3.0 (SC)), as well as CysD (Cg3115, \log_2 ratio -2.7 (PR)), a sulfate adenylyltransferase subunit involved in assimilatory sulfate reduction [69]. In contrast to these proteins, SufC (Cg1762, \log_2 ratio 0.5 (PR)) was slightly upregulated during growth on benzoate. The bacterial Suf proteins, studied for example in *E. coli*, constitute the iron sulfur cluster assembly machinery. SufC functions as an ATPase in this machinery [70].

4 Discussion

Previously, the cytoplasmic proteomes of *C. glutamicum* grown on five aromatic compounds were studied [42], giving insight into the aromatic degradation pathways and changes in the central carbon metabolism. However, scarce knowledge exists about the physiological adaptation of the membrane proteome during growth on aromatic carbon sources for bacteria in general and for *C. glutamicum* in particular. This fact motivated us to employ shotgun proteo-

Table 3. Results of an absolute protein quantification of BenE and BenK (for two biological replicates)

Absolute quantification of BenE and BenK						
Peptides:						
BenE	LASIAPPVAVAAVVGT[I]VAIASGK ^{a)}	Residues 187–210				
BenK	IGA[L]SAGAVGDR	Residues 74–85				
400 fmol/500 µg digested membrane proteins						
Biological replicate	Protein	No. of spectra analyzed	Mean ratio unlabeled/labeled	Standard deviation	Absolute amount [fmol]	Ratio BenE/BenK
1	BenE	24	0.29	0.02	116	
	BenK	10	0.15	0.01	60	1.93
3	BenE	168	0.99	0.10	398	
	BenK	33	0.70	0.06	280	1.41

a) Letters in brackets indicate the position of the labeled amino acid.

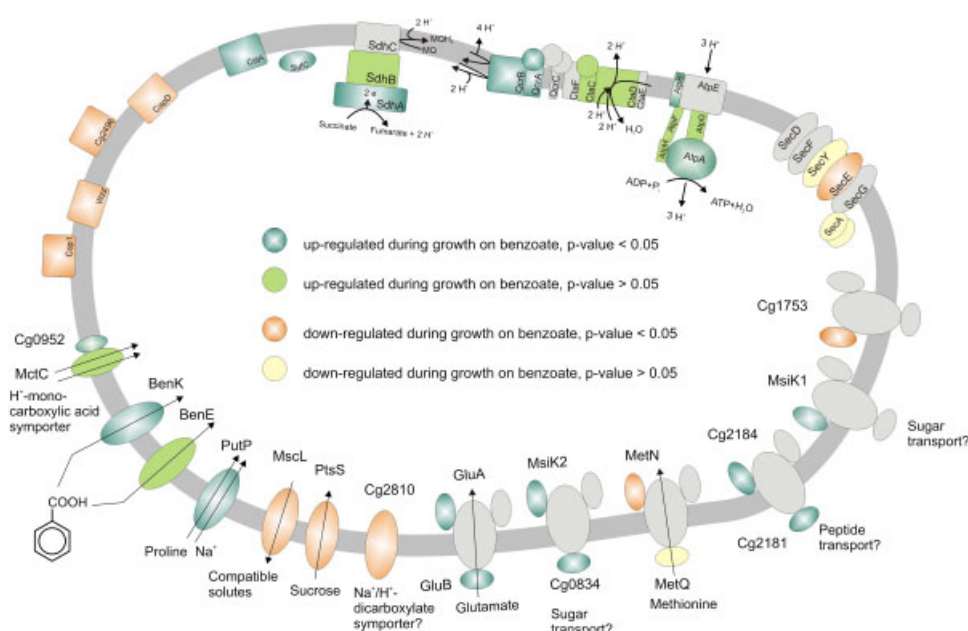


Figure 3. Summary of membrane-integral, secreted or membrane-associated proteins regulated during growth on benzoate or glucose (data from three biological replicates).

mics using the MudPIT/SIMPLE technology [21] combined with metabolic labeling, to obtain a quantitative survey of the membrane protein inventory. Discussion of results will focus on the co-expression of the two benzoate uptake proteins BenK and BenE, as well as on the adaptation of the central carbon and energy metabolism and the role of the McbR regulator in benzoate- and glucose-grown cells.

4.1 Benzoate transport

4.1.1 Benzoate transport proteins in *C. glutamicum*

C. glutamicum possesses two benzoate transport proteins, BenK and BenE. BenK belongs to the aromatic acid:H⁺

symporter family, a subfamily of the major facilitator superfamily (harboring 12 transmembrane helices) [71], to which the majority of aromatic acid transporters can be assigned [72]. BenE, in contrast, belongs to the benzoate:H⁺ symporter family [73] and differs in amino acid sequence and predicted secondary structure (11 transmembrane helices according to TMHMM [55]) from the major facilitator superfamily transporter proteins. Transcription analysis revealed that both benzoate transporters are transcribed simultaneously in the *C. glutamicum* strain RES167, although, as known so far, both transporters fulfill the same biological function, the uptake of benzoate [41]. Mutants, in which either one of the transporters is deleted, were still able to grow on benzoate as sole carbon source [41]. Still one might assume a second function for one or both of the

transporters, for example the uptake of benzoate derivatives or the export of either benzoate itself or some degradation intermediate.

Proteome analysis corroborates the results of the RT-PCR experiments, as both benzoate transporter proteins were identified in all biological replicates of the benzoate-grown cells. Results of the absolute quantification of the benzoate transporters indicated that BenE is slightly more abundant than BenK (factor of 1.4 to 1.9), thus, both benzoate transport proteins should substantially contribute to benzoate uptake in *C. glutamicum*.

A regulation-related difference between the two benzoate transporters cannot be ruled out, since only one growth condition was analyzed. However, both benzoate transporters are part of the same operon according to operon prediction in CoryneRegNet [54]. Recently, a GlxR binding site was detected upstream the transcription start site of *benK*. GlxR is assumed to repress transcription of the benzoate transporter genes [74]. The GlxR protein (Cg0350) was quantified in the predigest samples, but no significant change in abundance was detected between membranes of benzoate- and glucose-grown cells.

4.2 Comparison of *C. glutamicum* versus *Rhodococcus* sp. RHA1 and *Pseudomonas putida*

Rhodococcus sp. RHA1 (*Rhodococcus jostii* RHA1) is closely related to *C. glutamicum* and also possesses the two types of benzoate transporters. While *benK* (ro02388) is located adjacent to the *benABCD* gene cluster, *benE* (ro05524) is located separately from this cluster [75] unlike in *C. glutamicum*. In the *Rhodococcus* sp. RHA1 transcriptome on benzoate compared with pyruvate as sole carbon source, both benzoate transporter genes were upregulated during growth on benzoate, although upregulation was not statistically significant. [76]. Recently, one BenK homologue and two BenE homologues from *Pseudomonas putida* were functionally analyzed, revealing that all three proteins function as benzoate uptake systems [77].

4.3 Benzoate transport across the outer membrane

While BenK and BenE are located in the cytoplasmic membrane, it is unclear as to how the benzoate passes through the outer membrane of the *C. glutamicum* cell wall. If uncharged, benzoic acid should be able to diffuse across membranes, which may be impossible for the benzoate anion under our alkaline conditions (pH 8). Possibly, benzoate is transported into the periplasm *via* a porin, as BenF, a benzoate-specific porin, was identified in *Pseudomonas putida* [7]. Recently, a putative porin was identified in the outer membrane of *Pseudomonas* sp. strain phDV1,

however exclusively when grown on phenol and not on glucose [20]. In *C. glutamicum* no homologous protein exists to either BenF from *P. putida* or the putative porin from *Pseudomonas* sp. strain phDV1. All four *C. glutamicum* porins known so far (PorA, PorB, PorC, and PorH [78–80]) were identified in both benzoate- and glucose-grown cells; however, no differential regulation was detected for any of them.

4.4 Adaptation of the energy metabolism to benzoate

Growth on benzoate resulted in abundance differences for several proteins of the energy metabolism as well as for transport proteins (see Table 2). In *C. glutamicum*, benzoate is degraded *via* the β -keto adipate pathway yielding one molecule acetyl-CoA and one molecule succinyl-CoA. Therefore, cells grown on benzoate lack energy and reduction equivalents from glycolysis and partially from tricarboxylic acid cycle (TCA): One molecule of glucose yields 30 molecules of ATP [81], whereas one molecule of benzoate (according to our calculation) theoretically yields 15 ATP. The benzoate-grown cells exclusively depend on the TCA cycle and the oxidative phosphorylation for energy generation, leading to the upregulation of subunits of the succinate dehydrogenase, the cytochrome bc_1 -aa₃ supercomplex, and the ATP synthase. Similar observations were made in transcriptome analyses of acetate- [30] and citrate- [34] *versus* glucose-grown *C. glutamicum* cells: increases in mRNA levels were detected for *sdh* genes [30], genes coding for ATP synthase subunits, as well as *qcrB* (cg2403), coding for cytochrome B and *ctaE* (cg2406), coding for cytochrome C oxidase subunit 3 [34].

4.5 Impact of benzoate degradation on central carbon metabolism

4.5.1 Upregulation of benzoate-degrading enzymes

The first steps of benzoate degradation, its conversion to catechol, are catalyzed by enzymes encoded by the *ben* gene cluster (cg2637–cg2640), namely the benzoate 1,2-dioxygenase (BenABC) and the 1,6-dihydroxycyclohexa-2,4-diene-1-carboxylate-dehydrogenase (BenD). The α -subunit of the benzoate 1,2-dioxygenase, BenA, and BenD were found to be strongly upregulated in benzoate grown cells (\log_2 ratio 5.9 and 5.5, respectively). The putative regulator of the *ben* cluster, BenR (Cg2641), a transcriptional regulator of the LuxR family [37] also was significantly upregulated during growth on benzoate (\log_2 ratio 4.9). Possibly due to the high abundance of these cytoplasmic proteins in benzoate-grown cells, the benzoate-degrading enzymes were detected in the membrane fraction (in the predigest), too.

4.5.2 Regulation of TCA cycle enzymes corroborates previous findings

Besides the benzoate-degrading enzymes, other cytoplasmic enzymes involved in central carbon metabolism have been quantified in the membrane fraction (see Fig. 4). Although it cannot be completely ruled out that abundance changes of these proteins do not correspond to the cytoplasmic fraction, the regulation factors obtained for these proteins were compared to previous results of the analysis of the cytoplasmic proteome during growth on benzoate [42]. Upregulation of succinate dehydrogenase subunit A (Cg0446), catalyzing the reaction of succinate to fumarate, is consistent with the upregulation of fumarate hydratase (observed by Qi *et al.*), the enzyme catalyzing the next reaction in TCA cycle. Furthermore, the downregulation of aconitase (Cg1737, log₂ ratio -1.6, present study) is consistent with the downregulation of isocitrate lyase (observed by Qi *et al.*).

4.6 Indications for a starvation response

4.6.1 Upregulation of nutrient transport systems

Besides changes concerning the central carbon metabolism, several transport proteins changed their abundance during growth on benzoate: the proline transporter PutP (Cg1314) was upregulated in benzoate-grown cells. GluB (Cg2137; the secreted component) and GluA (the ATPase subunit of the glutamate uptake system)

were also upregulated during growth on benzoate. The GluABCD system is subject to catabolite repression by glucose [82], which is relieved during growth on benzoate. The enhanced abundance of these two amino acid transporters seems to reflect an increased demand for amino acids during growth on benzoate. As the TCA cycle and the oxidative phosphorylation provide the only source for energy generation, probably most benzoate degradation products are consumed for energy metabolism, leading to a decrease in amino acid biosynthesis. The upregulation of Cg2181 and Cg2184, annotated as subunits of an ABC-type peptide transport system, possibly also reflects the cells' demand for nutrients, although the specific substrates of this transporter are unknown so far. Additionally, MsiK1 (Cg2708) and MsiK2 (Cg0835), annotated as components of ATP-type sugar transport systems, were upregulated in benzoate-grown cells. Induction of an ABC-type sugar transporter during growth on benzoate also was reported for *Acinetobacter radioresistens* [2]. Therefore, not only the toxicity of benzoate could be responsible for retarded cell growth (own unpublished data), but also the cells' deficiency for nutrients and energy.

4.7 Parallels to the transcriptome of propionate-grown *C. glutamicum* cells

Concerning the regulated amino acid transport proteins, some remarkable parallels can be found in the study of

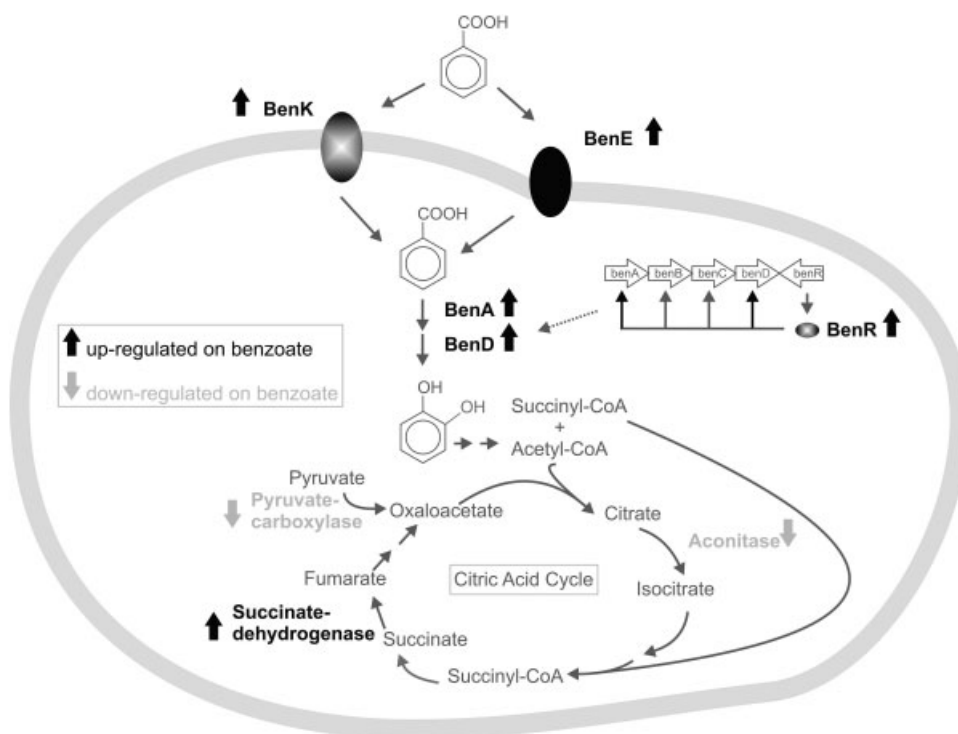


Figure 4. Overview of regulated proteins involved in benzoate transport and degradation and central carbon metabolism (data from three biological replicates).

Hüser *et al.* who compared the transcriptome of *C. glutamicum* ATCC 13032 grown on acetate and propionate with cells grown on acetate alone [31]:transcription of the genes *gluABCD*, *putP*, *cg2181*, and *cg2184* was upregulated during growth on acetate and propionate. Therefore, the abundance changes of these transport proteins in the present study probably reflect rather a general metabolic adaptation than a specific response to benzoate. Additionally, transcription of *cg0953* (forming an operon with *cg0952*) was upregulated during growth on propionate and acetate [31], and *Cg0952* was more abundant in benzoate-grown cells. Recently, *Cg0953* was characterized as monocarboxylic acid transporter (MctC) for pyruvate, acetate, and propionate [63].

4.8 Changes in sulfur metabolism – implications for differential regulation of McbR

4.8.1 Downregulation of McbR-regulated proteins

In contrast to PutP and the GluABCD system, the ATPase component of the methionine transport system, MetN was downregulated in benzoate-grown cells. The secreted component MetQ (*Cg0737*) exhibited the same regulation tendency (*p*-value > 0.05). As transporter of a sulfur-containing amino acid, the methionine transport system is linked to sulfur metabolism and directly regulated by McbR. McbR directly controls the transcription of 22 genes and operons and constitutes the master regulator of sulfur metabolism in *C. glutamicum* [83]. Like MetN, other proteins of the McbR regulon, such as the transcriptional regulator SsuR (*Cg0012*) and the enzymes MetK (*Cg1806*) and CysD (*Cg3115*), were downregulated during growth on benzoate.

4.9 Parallels to the transcriptome of a *C. glutamicum* Δ *mcbR* deletion mutant

In a transcriptome study of a *mcbR* deletion mutant, several genes, such as *cg0834*, *atpA* (*cg1366*), *cg2181*, *cg3195*, *cg0953* (*mctC*), and *cg2707*, showed reduced transcription in the mutant, probably due to indirect effects of McbR [83]. The corresponding gene products or proteins coded in the same operons were upregulated during growth on benzoate.

4.10 Is the differential regulation of McbR growth-dependent?

Regarding these parallels, McbR regulation seems to differ between benzoate- and glucose-grown cells. But it remains unclear as to how the exchange of the carbon source affects the sulfur metabolism of the cell. As *C. glutamicum* grows slower on benzoate than on glucose, the observed changes could be growth-dependent. On the other hand, proteins of

the McbR regulon (MetQ, MsiK1 (indirectly regulated)) were downregulated in gentisate-grown RES167 cells too (own unpublished data), although *C. glutamicum* is less retarded in its growth when grown on benzoate derivatives, such as gentisate or protocatechuate (own unpublished data). Additionally, instead of an upregulation of McbR during growth on benzoate, a downregulation of McbR under control conditions (glucose) should also be considered.

4.11 Does benzoate evoke organic acid stress in *C. glutamicum*?

Another reason for the changes concerning sulfur metabolism could be organic acid stress caused by benzoate. Roe *et al.* reported that growth inhibition of *E. coli* in the presence of weak organic acids was mainly due to an inhibition of methionine biosynthesis, leading to accumulation of homocysteine [84]. However, the fact that the *E. coli* experiments were conducted at an external pH of 6, which allows weak organic acids to pass the membrane in their protonated, uncharged form, should be considered. On the contrary, the growth medium for *C. glutamicum* was adjusted to pH 8, *i.e.* conditions where benzoate is deprotonated and thus unable to diffuse across the membrane.

5 Concluding remarks

The assimilation of benzoate instead of glucose by *C. glutamicum* leads to various physiological adaptations in the membrane. Both benzoate transport proteins, BenK and BenE, were expressed during growth on benzoate and the BenE:BenK ratio of 1.7 indicated that both proteins contribute substantially to benzoate transport. Concerning energy metabolism, benzoate induced increased abundance of proteins involved in oxidative phosphorylation, as well as a starvation response, which was expressed by upregulation of amino acid and putative sugar transport systems. Abundance changes of proteins involved in sulfur metabolism indicated a differential role of the global regulator McbR upon growth on benzoate and glucose. This study demonstrated that apart from the adaptation of central metabolic pathways, a global adaptation response can be observed in the membrane. This finding has promise for further research on membrane proteome adaptation to other aromatic compounds, as well as in further microbial species.

This work was supported by grants from the Bundesministerium für Bildung und Forschung (BMBF 0313812A), the Ruhr-University Research School funded by Germany's Excellence Initiative (DFG GSC 98/1) and the Deutsche Akademische Austausch Dienst (DAAD, D/05/06944).

The authors have declared no conflict of interest.

6 References

- [1] Giuffrida, M. G., Pessione, E., Mazzoli, R., Dellavalle, G. *et al.*, Media containing aromatic compounds induce peculiar proteins in *Acinetobacter radioresistens*, as revealed by proteome analysis. *Electrophoresis* 2001, 22, 1705–1711.
- [2] Pessione, E., Giuffrida, M. G., Prunotto, L., Barello, C. *et al.*, Membrane proteome of *Acinetobacter radioresistens* S13 during aromatic exposure. *Proteomics* 2003, 3, 1070–1076.
- [3] Park, S. H., Kim, J. W., Yun, S. H., Leem, S. H. *et al.*, Characterization of beta-ketoadipate pathway from multi-drug resistance bacterium, *Acinetobacter baumannii* DU202 by proteomic approach. *J. Microbiol.* 2006, 44, 632–640.
- [4] Zhao, B., Yeo, C. C., Lee, C. C., Geng, A. *et al.*, Proteome analysis of gentisate-induced response in *Pseudomonas alcaligenes* NCIB 9867. *Proteomics* 2004, 4, 2028–2036.
- [5] Kim, S. I., Kim, J. Y., Yun, S. H., Kim, J. H. *et al.*, Proteome analysis of *Pseudomonas* sp. K82 biodegradation pathways. *Proteomics* 2004, 4, 3610–3621.
- [6] Zhao, B., Yeo, C. C., Poh, C. L., Proteome investigation of the global regulatory role of sigma 54 in response to gentisate induction in *Pseudomonas alcaligenes* NCIMB 9867. *Proteomics* 2005, 5, 1868–1876.
- [7] Kim, Y. H., Cho, K., Yun, S. H., Kim, J. Y. *et al.*, Analysis of aromatic catabolic pathways in *Pseudomonas putida* KT 2440 using a combined proteomic approach: 2-DE/MS and cleavable isotope-coded affinity tag analysis. *Proteomics* 2006, 6, 1301–1318.
- [8] Zhao, B., Yeo, C. C., Tan, C. L., Poh, C. L., Proteome analysis of heat shock protein expression in *Pseudomonas alcaligenes* NCIMB 9867 in response to gentisate exposure and elevated growth temperature. *Biotechnol. Bioeng.* 2007, 97, 506–514.
- [9] Basu, A., Shrivastava, R., Basu, B., Apte, S. K., Phale, P. S., Modulation of glucose transport causes preferential utilization of aromatic compounds in *Pseudomonas putida* CSV86. *J. Bacteriol.* 2007, 189, 7556–7562.
- [10] Kim, S. J., Jones, R. C., Cha, C. J., Kweon, O. *et al.*, Identification of proteins induced by polycyclic aromatic hydrocarbon in *Mycobacterium vanbaalenii* PYR-1 using two-dimensional polyacrylamide gel electrophoresis and *de novo* sequencing methods. *Proteomics* 2004, 4, 3899–3908.
- [11] Liang, Y., Gardner, D. R., Miller, C. D., Chen, D. *et al.*, Study of biochemical pathways and enzymes involved in pyrene degradation by *Mycobacterium* sp. strain KMS. *Appl. Environ. Microbiol.* 2006, 72, 7821–7828.
- [12] Kim, S. J., Kweon, O., Jones, R. C., Freeman, J. P. *et al.*, Complete and integrated pyrene degradation pathway in *Mycobacterium vanbaalenii* PYR-1 based on systems biology. *J. Bacteriol.* 2007, 189, 464–472.
- [13] Kweon, O., Kim, S. J., Jones, R. C., Freeman, J. P. *et al.*, A polyomic approach to elucidate the fluoranthene-degradative pathway in *Mycobacterium vanbaalenii* PYR-1. *J. Bacteriol.* 2007, 189, 4635–4647.
- [14] Lee, S. E., Seo, J. S., Keum, Y. S., Lee, K. J., Li, Q. X., Fluoranthene metabolism and associated proteins in *Mycobacterium* sp. JS14. *Proteomics* 2007, 7, 2059–2069.
- [15] Patrauchan, M. A., Florizone, C., Dosanjh, M., Mohn, W. W. *et al.*, Catabolism of benzoate and phthalate in *Rhodococcus* sp. strain RHA1: redundancies and convergence. *J. Bacteriol.* 2005, 187, 4050–4063.
- [16] Navarro-Llorens, J. M., Patrauchan, M. A., Stewart, G. R., Davies, J. E. *et al.*, Phenylacetate catabolism in *Rhodococcus* sp. strain RHA1: a central pathway for degradation of aromatic compounds. *J. Bacteriol.* 2005, 187, 4497–4504.
- [17] Tomas-Gallardo, L., Canosa, I., Santero, E., Camafeita, E. *et al.*, Proteomic and transcriptional characterization of aromatic degradation pathways in *Rhodococcus* sp. strain TFB. *Proteomics* 2006, 6, S119–S132.
- [18] Patrauchan, M. A., Florizone, C., Eapen, S., Gomez-Gil, L. *et al.*, Roles of ring-hydroxylating dioxygenases in styrene and benzene catabolism in *Rhodococcus jostii* RHA1. *J. Bacteriol.* 2008, 190, 37–47.
- [19] Santoni, V., Molloy, M., Rabilloud, T., Membrane proteins and proteomics: un amour impossible? *Electrophoresis* 2000, 21, 1054–1070.
- [20] Papisotiriou, D. G., Markoutsas, S., Meyer, B., Papadioti, A. *et al.*, Comparison of the membrane subproteomes during growth of a new *pseudomonas* strain on lysogeny broth medium, glucose, and phenol. *J. Proteome Res.* 2008, 7, 4278–4288.
- [21] Fischer, F., Wolters, D., Rogner, M., Poetsch, A., Toward the complete membrane proteome: high coverage of integral membrane proteins through transmembrane peptide detection. *Mol. Cell Proteomics* 2006, 5, 444–453.
- [22] Oda, Y., Huang, K., Cross, F. R., Cowburn, D., Chait, B. T., Accurate quantitation of protein expression and site-specific phosphorylation. *Proc. Natl. Acad. Sci. USA* 1999, 96, 6591–6596.
- [23] Ong, S. E., Blagoev, B., Kratchmarova, I., Kristensen, D. B. *et al.*, Stable isotope labeling by amino acids in cell culture, SILAC, as a simple and accurate approach to expression proteomics. *Mol. Cell Proteomics* 2002, 1, 376–386.
- [24] Gygi, S. P., Rist, B., Gerber, S. A., Turecek, F. *et al.*, Quantitative analysis of complex protein mixtures using isotope-coded affinity tags. *Nat. Biotechnol.* 1999, 17, 994–999.
- [25] Ross, P. L., Huang, Y. N., Marchese, J. N., Williamson, B. *et al.*, Multiplexed protein quantitation in *Saccharomyces cerevisiae* using amine-reactive isobaric tagging reagents. *Mol. Cell Proteomics* 2004, 3, 1154–1169.
- [26] Liu, H., Sadygov, R. G., Yates, J. R., 3rd. A model for random sampling and estimation of relative protein abundance in shotgun proteomics. *Anal. Chem.* 2004, 76, 4193–4201.
- [27] Bridges, S. M., Magee, G. B., Wang, N., Williams, W. P. *et al.*, ProtQuant: a tool for the label-free quantification of MudPIT proteomics data. *BMC Bioinformatics* 2007, 8, S24.
- [28] Pan, C., Oda, Y., Lankford, P. K., Zhang, B. *et al.*, Characterization of anaerobic catabolism of *p*-coumarate in *Rhodopseudomonas palustris* by integrating transcriptomics and quantitative proteomics. *Mol. Cell Proteomics* 2008, 7, 938–948.

- [29] Eggeling, L., Sahm, H., L-Glutamate and L-lysine: traditional products with impetuous developments. *Appl. Microbiol. Biotechnol.* 1999, *52*, 146–153.
- [30] Muffler, A., Bettermann, S., Haushalter, M., Horlein, A. *et al.*, Genome-wide transcription profiling of *Corynebacterium glutamicum* after heat shock and during growth on acetate and glucose. *J. Biotechnol.* 2002, *98*, 255–268.
- [31] Huser, A. T., Becker, A., Brune, I., Dondrup, M. *et al.*, Development of a *Corynebacterium glutamicum* DNA microarray and validation by genome-wide expression profiling during growth with propionate as carbon source. *J. Biotechnol.* 2003, *106*, 269–286.
- [32] Arndt, A., Auchter, M., Ishige, T., Wendisch, V. F., Eikmanns, B. J., Ethanol catabolism in *Corynebacterium glutamicum*. *J. Mol. Microbiol. Biotechnol.* 2008, *15*, 222–233.
- [33] Silberbach, M., Schafer, M., Huser, A. T., Kalinowski, J. *et al.*, Adaptation of *Corynebacterium glutamicum* to ammonium limitation: a global analysis using transcriptome and proteome techniques. *Appl. Environ. Microbiol.* 2005, *71*, 2391–2402.
- [34] Polen, T., Schluesener, D., Poetsch, A., Bott, M., Wendisch, V. F., Characterization of citrate utilization in *Corynebacterium glutamicum* by transcriptome and proteome analysis. *FEMS Microbiol. Lett.* 2007, *273*, 109–119.
- [35] Kiefer, P., Heinzle, E., Zelder, O., Wittmann, C., Comparative metabolic flux analysis of lysine-producing *Corynebacterium glutamicum* cultured on glucose or fructose. *Appl. Environ. Microbiol.* 2004, *70*, 229–239.
- [36] Wittmann, C., Kiefer, P., Zelder, O., Metabolic fluxes in *Corynebacterium glutamicum* during lysine production with sucrose as carbon source. *Appl. Environ. Microbiol.* 2004, *70*, 7277–7287.
- [37] Brinkrolf, K., Brune, I., Tauch, A., Transcriptional regulation of catabolic pathways for aromatic compounds in *Corynebacterium glutamicum*. *Genet. Mol. Res.* 2006, *5*, 773–789.
- [38] Shen, X. H., Liu, Z. P., Liu, S. J., Functional identification of the gene locus *ncgl2319* and characterization of catechol 1,2-dioxygenase in *Corynebacterium glutamicum*. *Biotechnol. Lett.* 2004, *26*, 575–580.
- [39] Shen, X., Liu, S., Key enzymes of the protocatechuate branch of the beta-ketoadipate pathway for aromatic degradation in *Corynebacterium glutamicum*. *Sci. China C Life Sci.* 2005, *48*, 241–249.
- [40] Shen, X. H., Jiang, C. Y., Huang, Y., Liu, Z. P., Liu, S. J., Functional identification of novel genes involved in the glutathione-independent gentisate pathway in *Corynebacterium glutamicum*. *Appl. Environ. Microbiol.* 2005, *71*, 3442–3452.
- [41] Chaudhry, M. T., Huang, Y., Shen, X. H., Poetsch, A. *et al.*, Genome-wide investigation of aromatic acid transporters in *Corynebacterium glutamicum*. *Microbiology* 2007, *153*, 857–865.
- [42] Qi, S. W., Chaudhry, M. T., Zhang, Y., Meng, B. *et al.*, Comparative proteomes of *Corynebacterium glutamicum* grown on aromatic compounds revealed novel proteins involved in aromatic degradation and a clear link between aromatic catabolism and gluconeogenesis via fructose-1,6-bisphosphatase. *Proteomics* 2007, *7*, 3775–3787.
- [43] Poetsch, A., Wolters, D., Bacterial membrane proteomics. *Proteomics* 2008, *8*, 4100–4122.
- [44] Koch, D. J., Ruckert, C., Rey, D. A., Mix, A. *et al.*, Role of the *ssu* and *seu* genes of *Corynebacterium glutamicum* ATCC 13032 in utilization of sulfonates and sulfonate esters as sulfur sources. *Appl. Environ. Microbiol.* 2005, *71*, 6104–6114.
- [45] Liu, L., Wu, J. F., Ma, Y. F., Wang, S. Y. *et al.*, A novel deaminase involved in chloronitrobenzene and nitrobenzene degradation with *Comamonas* sp. strain CNB-1. *J. Bacteriol.* 2007, *189*, 2677–2682.
- [46] Kalinowski, J., Bathe, B., Bartels, D., Bischoff, N. *et al.*, The complete *Corynebacterium glutamicum* ATCC 13032 genome sequence and its impact on the production of L-aspartate-derived amino acids and vitamins. *J. Biotechnol.* 2003, *104*, 5–25.
- [47] Camon, E., Magrane, M., Barrell, D., Lee, V. *et al.*, The Gene Ontology Annotation (GOA) Database: sharing knowledge in Uniprot with gene ontology. *Nucleic Acids Res.* 2004, *32*, D262–D266.
- [48] Tauch, A., Kirchner, O., Löffler, B., Gotker, S. *et al.*, Efficient electrotransformation of *Corynebacterium diphtheriae* with a mini-replicon derived from the *Corynebacterium glutamicum* plasmid pGA1. *Curr. Microbiol.* 2002, *45*, 362–367.
- [49] Higdon, R., Hogan, J. M., Van Belle, G., Kolker, E., Randomized sequence databases for tandem mass spectrometry peptide and protein identification. *OMICS* 2005, *9*, 364–379.
- [50] Pan, C., Kora, G., McDonald, W. H., Tabb, D. L. *et al.*, ProRata: a quantitative proteomics program for accurate protein abundance ratio estimation with confidence interval evaluation. *Anal. Chem.* 2006, *78*, 7121–7131.
- [51] MacCoss, M. J., Wu, C. C., Liu, H., Sadygov, R., Yates, J. R., 3rd. A correlation algorithm for the automated quantitative analysis of shotgun proteomics data. *Anal. Chem.* 2003, *75*, 6912–6921.
- [52] Tabb, D. L., McDonald, W. H., Yates, J. R., 3rd. DTASelect and contrast: tools for assembling and comparing protein identifications from shotgun proteomics. *J. Proteome Res.* 2002, *1*, 21–26.
- [53] Wolfinger, R. D., Gibson, G., Wolfinger, E. D., Bennett, L. *et al.*, Assessing gene significance from cDNA microarray expression data via mixed models. *J. Comput. Biol.* 2001, *8*, 625–637.
- [54] Baumbach, J., CoryneRegNet 4.0 – a reference database for corynebacterial gene regulatory networks. *BMC Bioinformatics* 2007, *8*, 429.
- [55] Krogh, A., Larsson, B., von Heijne, G., Sonnhammer, E. L., Predicting transmembrane protein topology with a hidden Markov model: application to complete genomes. *J. Mol. Biol.* 2001, *305*, 567–580.
- [56] Xia, Q., Hendrickson, E. L., Wang, T., Lamont, R. J. *et al.*, Protein abundance ratios for global studies of prokaryotes. *Proteomics* 2007, *7*, 2904–2919.

- [57] Peter, H., Bader, A., Burkovski, A., Lambert, C., Kramer, R., Isolation of the *putP* gene of *Corynebacterium glutamicum* and characterization of a low-affinity uptake system for compatible solutes. *Arch. Microbiol.* 1997, **168**, 143–151.
- [58] Kronemeyer, W., Peekhaus, N., Kramer, R., Sahm, H., Eggeling, L., Structure of the *gluABCD* cluster encoding the glutamate uptake system of *Corynebacterium glutamicum*. *J. Bacteriol.* 1995, **177**, 1152–1158.
- [59] Trotschel, C., Follmann, M., Nettekoven, J. A., Mohrbach, T. *et al.*, Methionine uptake in *Corynebacterium glutamicum* by MetQNI and by MetPS, a novel methionine and alanine importer of the NSS neurotransmitter transporter family. *Biochemistry* 2008, **47**, 12698–12709.
- [60] Nottebrock, D., Meyer, U., Kramer, R., Morbach, S., Molecular and biochemical characterization of mechanosensitive channels in *Corynebacterium glutamicum*. *FEMS Microbiol. Lett.* 2003, **218**, 305–309.
- [61] Moker, N., Brocker, M., Schaffer, S., Kramer, R. *et al.*, Deletion of the genes encoding the MtrA-MtrB two-component system of *Corynebacterium glutamicum* has a strong influence on cell morphology, antibiotics susceptibility and expression of genes involved in osmoprotection. *Mol. Microbiol.* 2004, **54**, 420–438.
- [62] Brocker, M., Bott, M., Evidence for activator and repressor functions of the response regulator MtrA from *Corynebacterium glutamicum*. *FEMS Microbiol. Lett.* 2006, **264**, 205–212.
- [63] Jolkver, E., Emer, D., Ballan, S., Kramer, R. *et al.*, Identification and characterization of a bacterial transport system for the uptake of pyruvate, propionate, and acetate in *Corynebacterium glutamicum*. *J. Bacteriol.* 2009, **191**, 940–948.
- [64] Brand, S., Niehaus, K., Puhler, A., Kalinowski, J., Identification and functional analysis of six mycolyltransferase genes of *Corynebacterium glutamicum* ATCC 13032: the genes *cop1*, *cmt1*, and *cmt2* can replace each other in the synthesis of trehalose dicorynomycolate, a component of the mycolic acid layer of the cell envelope. *Arch. Microbiol.* 2003, **180**, 33–44.
- [65] Franco, A. V., Liu, D., Reeves, P. R., The *wzz* (*clD*) protein in *Escherichia coli*: amino acid sequence variation determines O-antigen chain length specificity. *J. Bacteriol.* 1998, **180**, 2670–2675.
- [66] Candela, T., Fouet, A., *Bacillus anthracis* CapD, belonging to the gamma-glutamyltranspeptidase family, is required for the covalent anchoring of capsule to peptidoglycan. *Mol. Microbiol.* 2005, **57**, 717–726.
- [67] Grossmann, K., Herbster, K., Mack, M., Rapid cloning of *metK* encoding methionine adenosyltransferase from *Corynebacterium glutamicum* by screening a genomic library on a high density colony-array. *FEMS Microbiol. Lett.* 2000, **193**, 99–103.
- [68] Koch, D. J., Ruckert, C., Albersmeier, A., Huser, A. T. *et al.*, The transcriptional regulator SsuR activates expression of the *Corynebacterium glutamicum* sulphionate utilization genes in the absence of sulphate. *Mol. Microbiol.* 2005, **58**, 480–494.
- [69] Ruckert, C., Koch, D. J., Rey, D. A., Albersmeier, A. *et al.*, Functional genomics and expression analysis of the *Corynebacterium glutamicum* *fpr2-cyslXHDNYZ* gene cluster involved in assimilatory sulphate reduction. *BMC Genomics* 2005, **6**, 121.
- [70] Kitaoka, S., Wada, K., Hasegawa, Y., Minami, Y. *et al.*, Crystal structure of *Escherichia coli* SufC, an ABC-type ATPase component of the SUF iron-sulfur cluster assembly machinery. *FEBS Lett.* 2006, **580**, 137–143.
- [71] Pao, S. S., Paulsen, I. T., Saier, M. H., Jr. Major facilitator superfamily. *Microbiol. Mol. Biol. Rev.* 1998, **62**, 1–34.
- [72] Parales, R. E., Ju, K. S., Rollefson, J. B., Ditty, J. L., in: Diaz, E. (Ed.), *Microbial Biodegradation: Genomics and Molecular Biology*, Caister Academic Press, Norfolk, UK 2008, pp. 145–187.
- [73] Saier, M. H., Jr., Tran, C. V., Barabote, R. D., TCDB: the Transporter Classification Database for membrane transport protein analyses and information. *Nucleic Acids Res.* 2006, **34**, D181–D186.
- [74] Kohl, T. A., Baumbach, J., Jungwirth, B., Puhler, A., Tauch, A., The GlxR regulon of the amino acid producer *Corynebacterium glutamicum*: *in silico* and *in vitro* detection of DNA binding sites of a global transcription regulator. *J. Biotechnol.* 2008, **135**, 340–350.
- [75] McLeod, M. P., Warren, R. L., Hsiao, W. W., Araki, N. *et al.*, The complete genome of *Rhodococcus* sp. RHA1 provides insights into a catabolic powerhouse. *Proc. Natl. Acad. Sci. USA* 2006, **103**, 15582–15587.
- [76] Goncalves, E. R., Hara, H., Miyazawa, D., Davies, J. E. *et al.*, Transcriptomic assessment of isozymes in the biphenyl pathway of *Rhodococcus* sp. strain RHA1. *Appl. Environ. Microbiol.* 2006, **72**, 6183–6193.
- [77] Nishikawa, Y., Yasumi, Y., Noguchi, S., Sakamoto, H., Nikawa, J., Functional analyses of *Pseudomonas putida* benzoate transporters expressed in the yeast *Saccharomyces cerevisiae*. *Biosci. Biotechnol. Biochem.* 2008, **72**, 2034–2038.
- [78] Costa-Riu, N., Maier, E., Burkovski, A., Kramer, R. *et al.*, Identification of an anion-specific channel in the cell wall of the Gram-positive bacterium *Corynebacterium glutamicum*. *Mol. Microbiol.* 2003, **50**, 1295–1308.
- [79] Costa-Riu, N., Burkovski, A., Kramer, R., Benz, R., PorA represents the major cell wall channel of the Gram-positive bacterium *Corynebacterium glutamicum*. *J. Bacteriol.* 2003, **185**, 4779–4786.
- [80] Hunten, P., Schiffler, B., Lottspeich, F., Benz, R., PorH, a new channel-forming protein present in the cell wall of *Corynebacterium efficiens* and *Corynebacterium callunae*. *Microbiology* 2005, **151**, 2429–2438.
- [81] Berg, J. M., Tymoczko, J. L., Stryer, L., *Biochemistry*, W.H. Freeman, New York 2007.
- [82] Kramer, R., Lambert, C., Hoischen, C., Ebbighausen, H., Uptake of glutamate in *Corynebacterium glutamicum*. 1. Kinetic properties and regulation by internal pH and potassium. *Eur. J. Biochem.* 1990, **194**, 929–935.
- [83] Rey, D. A., Nentwich, S. S., Koch, D. J., Ruckert, C. *et al.*, The McbR repressor modulated by the effector substance

- S-adenosylhomocysteine controls directly the transcription of a regulon involved in sulphur metabolism of *Corynebacterium glutamicum* ATCC 13032. *Mol. Microbiol.* 2005, *56*, 871–887.
- [84] Roe, A. J., O'Byrne, C., McLaggan, D., Booth, I. R., Inhibition of *Escherichia coli* growth by acetic acid: a problem with methionine biosynthesis and homocysteine toxicity. *Microbiology* 2002, *148*, 2215–2222.
- [85] Sugawara, H., Abe, T., Gojobori, T., Tateno, Y., DDBJ working on evaluation and classification of bacterial genes in INSDC. *Nucleic Acids Res.* 2007, *35*, D13–D15.
- [86] Lane, D. J., in: Stackebrandt, E., Goodfellow, M. (Eds.), *Nucleic Acid Techniques in Bacterial Systematics*, John Wiley & Sons, New York 1991, pp. 115–148.